Monthly Notices
of the
ROYAL ASTRONOMICAL SOCIETY

MNRAS **466,** 3600–3611 (2017)
Advance Access publication 2016 December 22

doi:10.1093/mnras/stw3284

Low-redshift quasars in the SDSS Stripe 82: associated companion galaxies and signature of star formation

D. Bettoni,[1]★ R. Falomo,[1]★ J. K. Kotilainen[2,3]★ and K. Karhunen[3]

[1]*INAF – Osservatorio Astronomico di Padova, Vicolo dell'Osservatorio 5, I-35122 Padova (PD), Italy*
[2]*Finnish Centre for Astronomy with ESO (FINCA), University of Turku, Väisäläntie 20, FI-21500 Piikkiö, Finland*
[3]*Tuorla Observatory, Department of Physics and Astronomy, University of Turku, FI-21500 Piikkio, Finland.*

Accepted 2016 December 14. Received 2016 December 14; in original form 2016 September 1

ABSTRACT

We obtained optical spectroscopy of close (<80 kpc) companion objects of a sample of 12 low-redshift quasars ($z < 0.3$) selected from the SDSS Stripe82 area and that are in the subsample of 52 QSOs for which both multicolour host galaxies properties and galaxy environment were recently investigated in detail. We found that for 8 out of 12 sources the companion galaxy is associated with the QSO having a difference of radial velocity that is less than 400 km s^{-1}. Many of these associated companions exhibit [O II] λ3727 Å emission lines suggestive of episodes of (recent) star formation possibly induced by past interactions. The star formation rate of the companion galaxies as derived from [O II] line luminosity is, however, modest, with a median value of 1.0 ± 0.8 $M_{\odot}$ yr^{-1}, and the emission lines are barely consistent with expectation from gas ionization by the QSO. The role of the QSO for inducing star formation in close companion galaxies appears meager. For three objects we also detect the starlight spectrum of the QSO host galaxy, which is characterized by absorption lines of old stellar population and [O II] emission line.

Key words: galaxies: active – galaxies: evolution – galaxies: nuclei – quasars: general.

1 INTRODUCTION

Active supermassive black holes (quasars, QSO) are rare objects in the Universe but they represent a key ingredient to fully understand the processes that have built the galaxies. In fact, a general consensus has emerged in the last decade that all sufficiently massive galaxies have a massive black hole in their centre and therefore have the possibility to shine as a quasar. In spite of several studies aimed to understand the mechanisms that activate and fuel the active nuclei of galaxies only fragmented data are available. The most accredited responsible for transforming a dormant massive black hole into a luminous quasar remains dissipative tidal interactions and galaxy merging. Minor and major merging events may have a key role for triggering and fueling the nuclear/quasar activity. These effects strictly depend on the global properties of the galaxy environment (see e.g. Kauffmann & Haehnelt 2000; Di Matteo, Springel & Hernquist 2005).

At low redshift quasars follow the large-scale structure traced by galaxy clusters but they eschew the very centre of clusters (Söchting, Clowes & Campusano 2002, 2004). On the other hand, on small scales (projected distance < 1 Mpc), the quasar environment appears overpopulated by blue disc galaxies having a strong star formation rate (SFR; Coldwell & Lambas 2003, 2006). However, at Mpc scale, comparing the environments of quasars to those of galaxies has given conflicting results. Early studies on scales of 10 Mpc suggest that quasars are more strongly clustered than galaxies (see e.g. Shanks, Boyle & Peterson 1988), while later studies based on surveys such as the Two Degree Field and the SDSS have found that the galaxy densities of quasars and inactive galaxies are comparable (see e.g. Smith, Boyle & Maddox 2000; Wake et al. 2004; Serber et al. 2006; Matsuoka et al. 2014).

Since early imaging studies of the QSOs and their environments it was noted that in a number of cases companion galaxies were found close to the quasars (Stockton 1982; Hutchings & Neff 1992). Further investigations were carried out using narrow band images that were tuned to detect strong emission-line (mainly [O II] 3727 Å and [O III] 4959, 5007 Å) companions at the rest-frame redshift of the QSOs (e.g. Hutchings, Crampton & Persram 1993; Hutchings 1995b; Hutchings, Crampton & Johnson 1995a; Hutchings & Morris 1995). These observations of close companion galaxies are thus suggestive of a physical association with the quasars (Stockton & MacKenty 1987). A more sound proof of the association between the QSO and a close companion galaxy comes from the accurate spectroscopic measurement of both their redshifts. Examples of these association are shown by Hutchings & Neff (1992) and became more evident by *Hubble Space Telescope* images (e.g. Bahcall et al. 1997 for low-z objects and by high-quality images obtained in the near-IR for high-z sources (e.g. Falomo et al. 2001, 2008). Recently further spectroscopic evidence of this was given by

★ E-mail: daniela.bettoni@oapd.inaf.it (DB); renato.falomo@oapd.inaf.it (RF); jarkot@utu.fin (JKK)

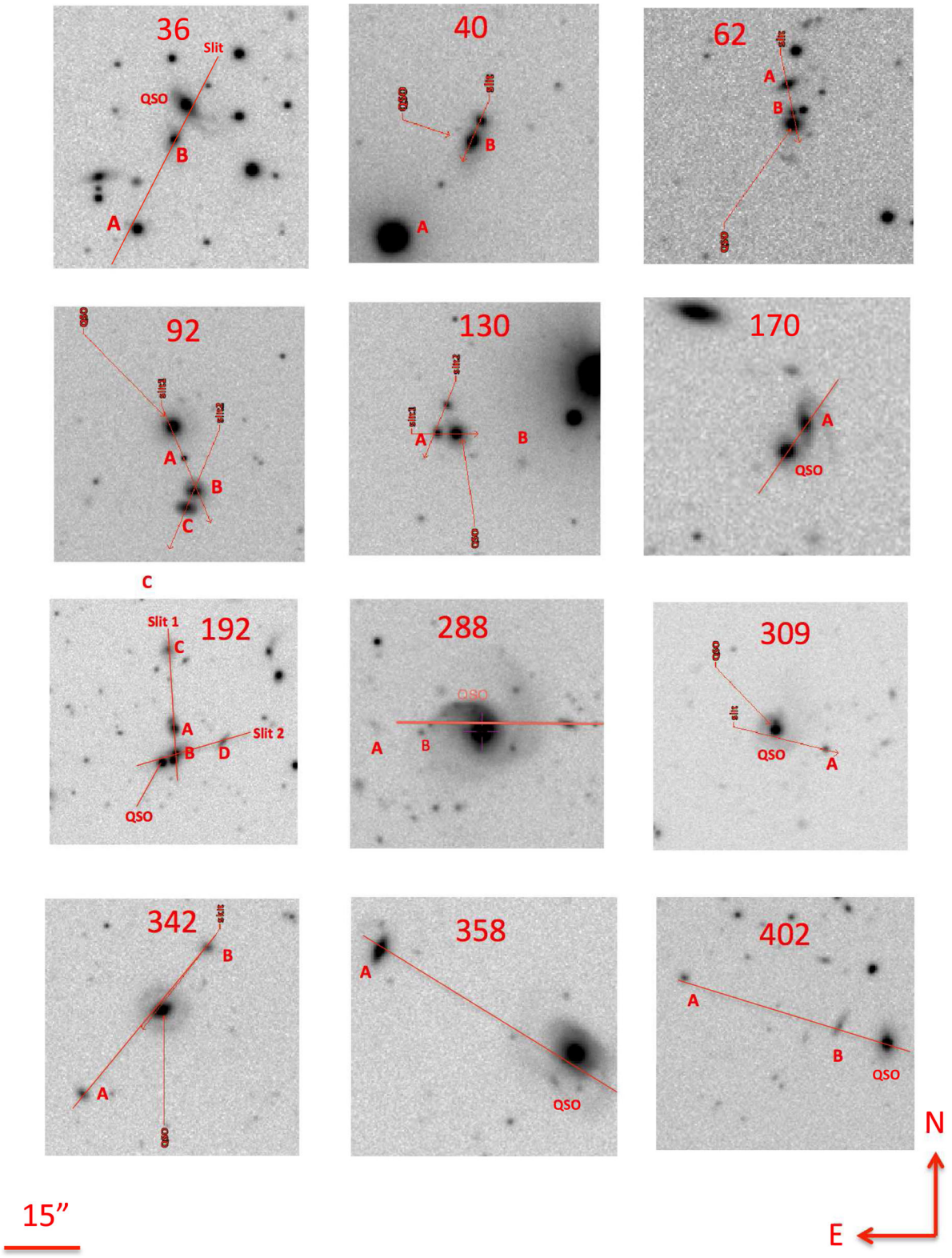

Figure 1. SDSS images (*i* filter) of the field around the QSO showing the companion galaxies for which spectra were secured (see also Table 1). The adopted slit positions are shown by a red solid line.

Villar-Martín et al. (2011) for a small sample of low-redshift QSOs.

These companion galaxies of quasars could be the product of a major merger of galaxies that led to the nuclear activities of QSOs (Stockton 1982; Bekki 1999). It is therefore of interest to investigate by spectroscopy these close companions in order to prove their physical association with the QSO and to search for signature of recent star formation. Either these issues can probe and eventually

Table 1. The observed QSO and companion galaxies.

Nr	Obj	SDSSJ	z_{SDSS}	PD (kpc)	PA (°)	offset (arcsec)	*u*	*g*	*r*	*i*	*z*
36	QSO	211234.88−005926.8	0.2351			1.8	18.73	18.71	18.37	17.96	17.83
	Obj. A	211235.72−005958.9		130.1	155	2.5	19.42	18.22	17.75	17.58	17.49
	Gal. B	211235.08−005935.7		53.1	155		22.54	20.48	19.08	18.50	18.20
40	QSO	211832.75+004500.8	0.2332			1.35	18.69	18.60	18.34	17.94	17.91
	Gal. B	211832.62+004505.4		27.9	150		22.14	20.81	19.95	19.13	18.95
62	QSO	215744.18+005303.6	0.2674				18.66	18.63	18.44	18.35	17.91
	Gal. B	215744.26+005313.8		67.4	10		24.79	21.24	19.66	19.11	18.67
92	QSO	222632.66−005717.7	0.1681			1.3	17.89	17.87	17.64	17.27	17.21
	Gal. A	222632.46−005726.3		35.5	25		23.69	24.16	21.68	19.94	18.88
	Gal. B	222632.27−005735.3		72.2	150		20.04	18.87	18.08	17.61	17.31
	Gal. C	222632.40−005739.8		87.3	150		20.59	19.35	18.67	18.27	17.92
130	QSO	231711.79−003603.6	0.1861			1.0	17.81	17.97	17.82	17.40	17.48
	Gal. A	231712.12−003603.5		21.7	12		23.45	20.72	19.58	19.22	18.88
	Gal. B	231710.52−003603.8		82.5	12		25.29	22.78	22.64	21.18	22.87
	Gal. C	231711.95−003555.8		35.5	152		21.25	20.37	19.72	19.46	19.44
170	QSO	000557.23+002837.7	0.2596				18.59	18.57	18.41	18.37	17.86
	Gal. B	000557.04+002842.2		34.2	160		21.55	19.84	18.67	18.11	17.76
192	QSO	002831.71−000413.3	0.2519				18.33	17.99	17.67	17.38	17.11
	Gal. A	002831.40−000400.8		81.2	15		20.11	19.32	18.58	18.14	17.95
	Gal. B	002831.36−000409.9		37.9	120		22.57	20.80	18.50	18.04	17.57
	Gal. C	002831.57−000332.7		244.4	15		21.18	20.20	19.44	19.11	19.12
	Gal. D	J002830.16−000405.8		145.4	120		26.38	22.11	20.44	19.87	19.54
288	QSO.	015950.24+002340.8	0.1627				15.91	15.90	15.96	15.73	15.82
	Gal. B	015951.11+002342.8		49.2	0		23.04	21.70	21.26	22.81	20.94
309	QSO	021359.79+004226.7	0.1823				17.67	17.67	17.33	16.90	17.19
	Gal. A	021358.87+004221.3		62.72	20		23.49	21.87	20.63	20.16	19.70
342	QSO	025334.57+000108.3	0.1705			1.3	19.01	18.52	18.07	17.57	17.29
	Gal. A	025336.01+000045.6		123.1	142		21.86	20.60	20.01	19.59	19.71
	Gal. B	025333.76+000125.2		82.3	142		20.46	19.79	19.48	19.31	19.18
358	QSO	030639.57+000343.1	0.1074			2.3	17.72	17.34	17.11	16.59	16.55
	Gal. A	030642.89+000409.6		132.5	65		20.65	18.64	17.63	17.18	16.78
402	QSO	033651.52−001024.7	0.1868				18.58	18.57	18.22	17.76	17.63
	Gal. A	033652.31−001019.8		56.2	65		24.69	22.03	20.44	19.88	19.07

Column (1) identifier from Falomo et al. (2014), column (2) the QSO galaxy identifier, columns (3) and (4) the name and redshift from SDSS, Column (5) PD the Projected Distance of the companion in kpc, column (6) the observed position angle (PA), column (7) the slit offset from the QSO nucleus, columns (8) to (12) the *u*, *g*, *r*, *i* and *z* magnitudes from SDSS−DR7.

support the hypothesis that merging of galaxies is linked to the fueling and triggering of powerful nuclear activity in galaxies.

We have recently carried out an imaging study of the close companions around ∼50 low-redshift ($z < 0.3$) quasars (Bettoni et al. 2015). The targets were extracted from a larger data set of approximately 400 quasars at $z < 0.5$ for which both the host galaxies and their galaxy environments were studied (Falomo et al. 2014; Karhunen et al. 2014) based on deep multicolour images of the SDSS Stripe82 (Annis et al. 2014). It was found that for about 60 per cent of the QSOs there is a companion galaxy at projected distance (PD) less than 50 kpc, and for half of them there are two or more companions. The comparison with a sample of inactive galaxies of comparable luminosity and at similar redshift of the QSO hosts yields analogous results suggesting a weak link between the presence of close companions and nuclear activity. However, we found an indication that bright companion galaxies are a factor of 2 more frequent in QSO than in inactive galaxies (Bettoni et al. 2015).

In order to better understand the connection between nuclear activity and interaction/merging phenomena, we should identify which companion galaxies are physically connected to the QSO (same redshift) from those that are just projected. Unfortunately, only in few cases the redshift of these companions was available from the SDSS spectroscopy and as expected some of these companions are found to be not physically associated with the QSO (the companions are mainly foreground galaxies) thus hampering a sound interpretation of the effect of close companion galaxies on the nuclear activity. As a further step in this study, we have therefore obtained spectroscopy of the companion galaxies of the QSO in the above sample in order to probe their physical association and to search for signature of recent star formation.

The paper is organized as follows: in Section 2, we present our QSO sample. Section 3 describes the analysis of the data and the main properties of the host galaxies and in Section 4, we discuss our results and we compare our findings with those of Matsuoka et al. (2014). We adopt the concordance cosmology with $H_0 = 70$ km s^{-1} Mpc^{-1}, $\Omega_m = 0.3$ and $\Omega_\Lambda = 0.7$.

2 THE SAMPLE

The targets are extracted from the sample of 52 low-redshift ($z < 0.3$) quasars for which we carried out a multicolour study of their host galaxies and close environments (Bettoni et al. 2015). These targets belong to a larger data set of ∼ 400 quasars ($z < 0.5$) located in the SDSS-Stripe82 (Abazajian et al. 2009; Annis et al. 2014) that was extensively investigated for the environment and host galaxy properties in our previous works (Falomo et al. 2014; Karhunen

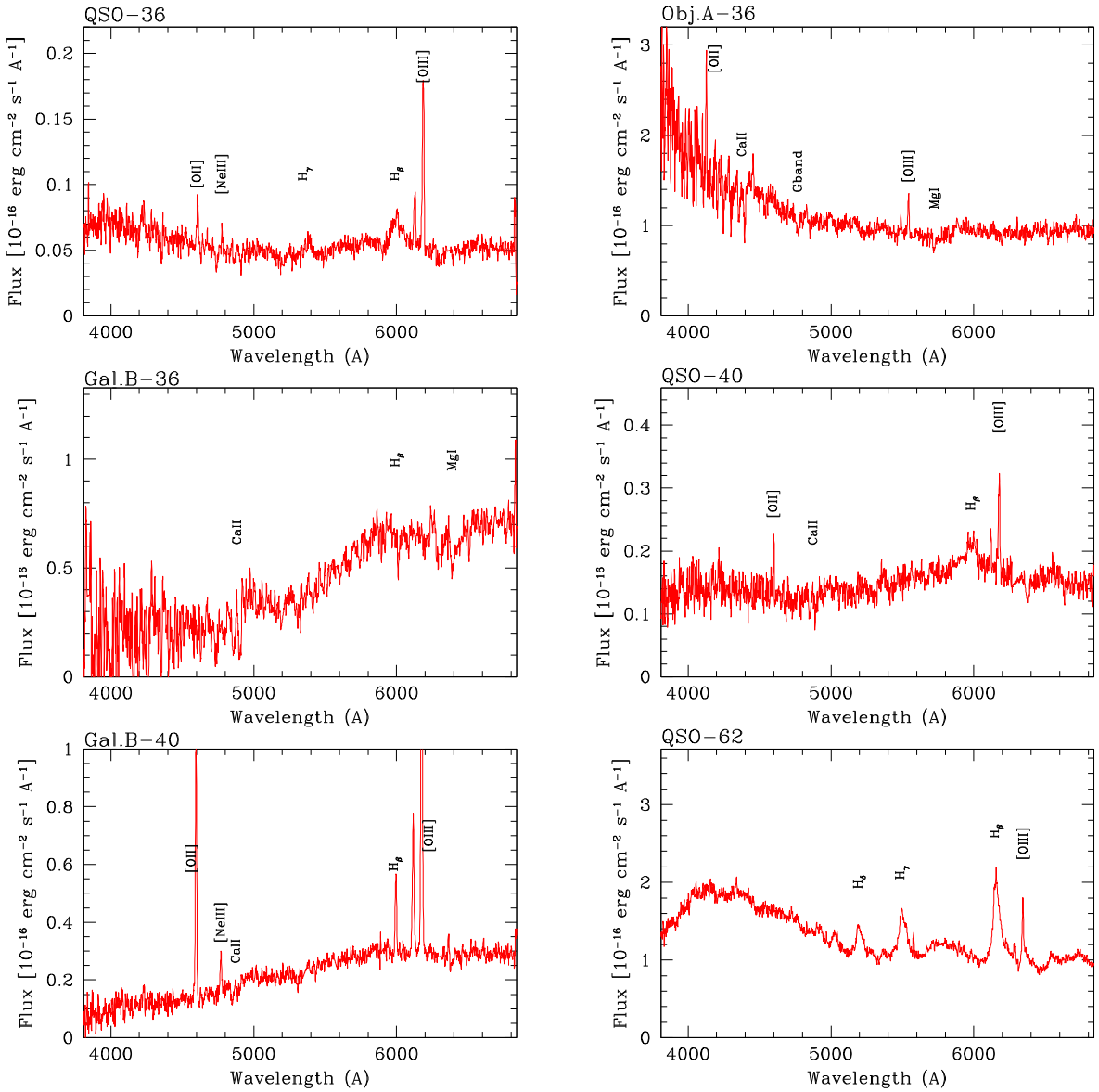

Figure 2. Optical spectra of QSO and their close companion galaxies (see also 1). Main emission and/or absorptions lines are marked by labels.

et al. 2014; Karhunen et al., in preparation; Bettoni et al. 2015). We selected 18 QSOs with $z < 0.3$ for which the host galaxy is well resolved (see details in Falomo et al. 2014) and for each objects of this sample there is at least one close (distance ≤ 80 kpc) companion galaxy with an apparent r-band magnitude brighter than $r = 22$. In order to test the possible association with the QSO, we obtained optical spectra of both the host galaxy and the close companion using the slit aligned along the two objects (see in Fig. 1 the fields of view of our targets). Due to the observing conditions, we could observe only 12 objects (i.e. 67 per cent) of the whole selected sample. In Table 1, we give the list of the observed QSOs and their main properties. For this subsample of QSO, we obtained off-nuclear spectra of QSO hosts and of the close companions.

3 OBSERVATIONS AND DATA ANALYSIS

The spectra of the QSO and of the close companions were collected with the Nordic Optical Telescope at La Palma. Observations were performed with grism #7 on ALFOSC, this give a spectral resolution of $R = 500$, with the used slit, 1.3 arcsec wide. Our targets were observed in two different runs in 2015 September 13–16 and November 9–12. For each QSO the slit was oriented slightly offset (1–2 arcsec corresponding to 4–10 kpc at the redshift of the targets) from the QSO nucleus and at a position angle (PA) that allows us to take the spectra of the companion simultaneously. In Table 1, for each QSO, we give the observed PAs and offsets from the nucleus.

Standard IRAF[1] tools were adopted for the data reduction. Bias subtraction, flat-field correction, image alignment and combination were performed. Cosmic rays were cleaned by combining different exposures with the *crreject* algorithm. The spectra were then calibrated both in wavelength and in flux. The accuracy of the wavelength calibrations is ∼0.2 Å. Since only a fraction of the flux from the companion galaxies is gathered through the slit we have

[1] IRAF is distributed by the National Optical Astronomy Observatory, which is operated by the Association of Universities for Research in Astronomy under cooperative agreement with the National Science Foundation.

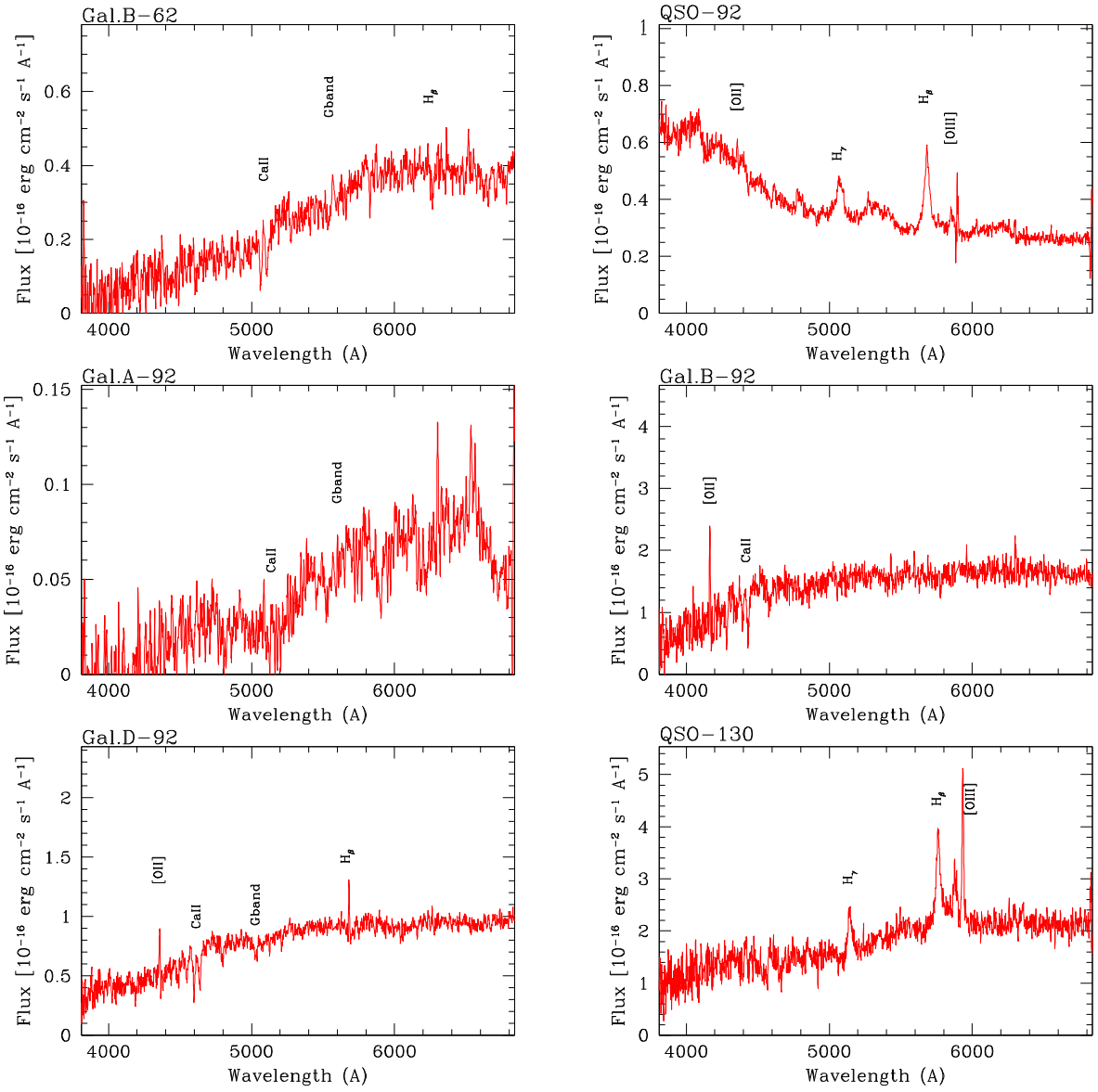

Figure 2 – *continued.*

set the absolute flux calibration of the spectra by normalizing the continuum to the flux corresponding to the *r*-band magnitude of the galaxy as derived from the same SDSS images used in Falomo et al. (2014). In the case of the spectra of the QSO host galaxies, we instead normalized the flux of their spectra to the total magnitude of the host galaxies as derived in our previous study of the QSO hosts for the whole sample (Falomo et al. 2014). The final spectra are presented in Fig. 2.

We used the RVSAO IRAF package to measure the redshift, both for emission (with *emsao*) and pure absorption spectra (with *xcsao*). In the case of absorption line spectra, we used as template a synthetic stellar spectrum (a KIII star) taken from the Jacoby, Hunter & Christian (1984) library. In Table 2, we give our measured redshift.

4 RESULTS

In Fig. 2, we report the optical spectra of the 12 observed quasars and of their companion galaxies. Results from the spectra of the companion objects are summarized in Table 2 and specific comments on individual objects given in the Appendix. In a number of cases, there is more than one companion inside the slit, thus in total we are able to secure the spectra of 22 objects in the immediate environment around the targets. It turned out that 1 out of these 22 apparent companions is a star (object labelled A for QSO 40) and is not furthermore considered in this work (see Fig. 1). Thus, the final sample of analysed spectra is composed of 21 galaxies.

4.1 Close companion galaxies

We found that for eight QSO the selected companion galaxy at PD < 80 kpc is associated with the quasars (assuming $\Delta V < 400$ km sec^{-1}), while in the remaining four cases, the companions are either a foreground or a background galaxy. In one (no. 192) out of the eight cases, where we have one associated companion galaxy, there is another companion galaxy at PD larger than 80 kpc that is at the same redshift of the QSO. In another one(#130), two more associated companion galaxies are found. One of the three companion objects is a very faint galaxy

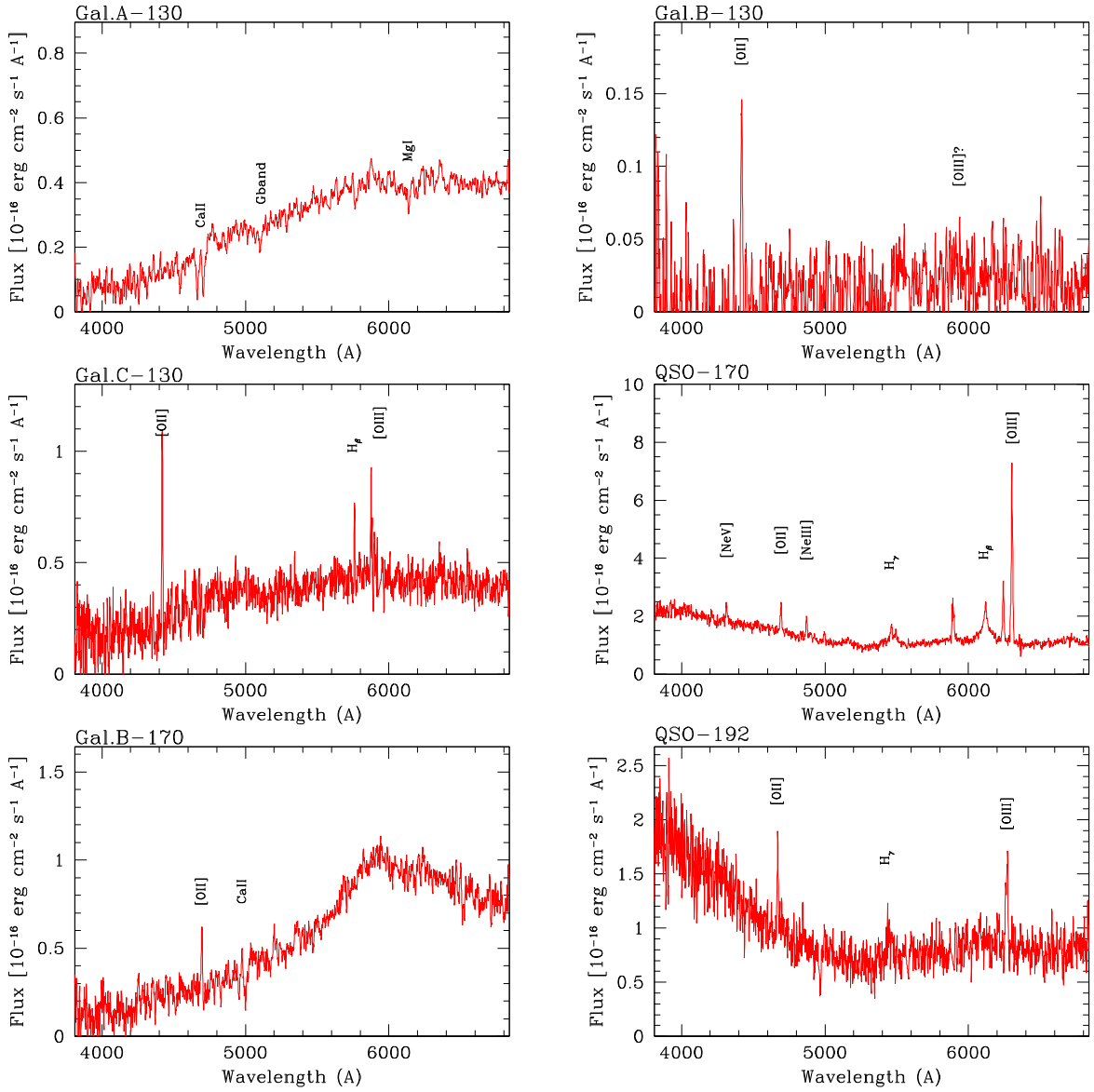

Figure 2 – *continued.*

($M_i \sim -18.6$), almost undetectable in the broad-band Stripe82 images but with clear visible [O II] and [O III] emission lines in the spectrum (see Figs 2 and 3). The total number of companions turn out to be 11.

In Fig. 4, we show the distribution of ΔV (the difference of radial velocity between the companion galaxy and the QSO) with respect to the PD of the associated companion galaxies. Closer companions are found to have also the smallest ΔV.

4.2 Star formation from [O II] lines

For 20 (9 QSOs and 11 galaxies in the fields) out of 33 observed sources, we detect a significant emission line of [OII] 3727 Å. Only 5 of the 11 galaxies with [OII] 3727 emission are associated with the QSO and are used in our analysis but for completeness in Table 2 we report the values for the non-associated companions for comparison. The intensity of this line can be used as an approximate tracer of the SFR (e.g. Gallagher, Hunter & Bushouse 1989; Kennicutt 1998) because the relationship between [O II] luminosity and SFR may be affected by reddening and relative abundance. The observed [O II] luminosity ranges from 10^{39} to 2×10^{41} erg s^{-1} with the exception of QSO 288 that exhibits an [O II] luminosity $>10^{42}$ erg s^{-1}. On average, these luminosities cover the faint tail of the $L_{[O\,II]}$ luminosity of the QSO (Kalfountzou et al. 2012). In Table 2, we report the intensity and the luminosity of the measured [OII] emission lines for all observed galaxies. To estimate the SFR, we adopt the recipe proposed by Gilbank et al. (2010) (their equation 8; see also Gilbank et al. 2011) that takes in to account, in an empirical form, the systematic effects of mass (metallicity) for the SFR versus [O II] luminosity relationship. The mass of the galaxies for which we secure the spectra was estimated using the empirical relationship between stellar mass, absolute magnitude and colour derived by Kauffmann et al. (2003) and Gilbank et al. (2010) from multicolour SDSS imaging of a very large sample of low-redshift ($z \sim 0.1$) galaxies. The stellar masses of our galaxies were derived using the SDSS magnitudes and applying k-correction using the routine KCORRECT (Blanton & Roweis 2007) for consistency with the derived empirical relation. The values for the masses and

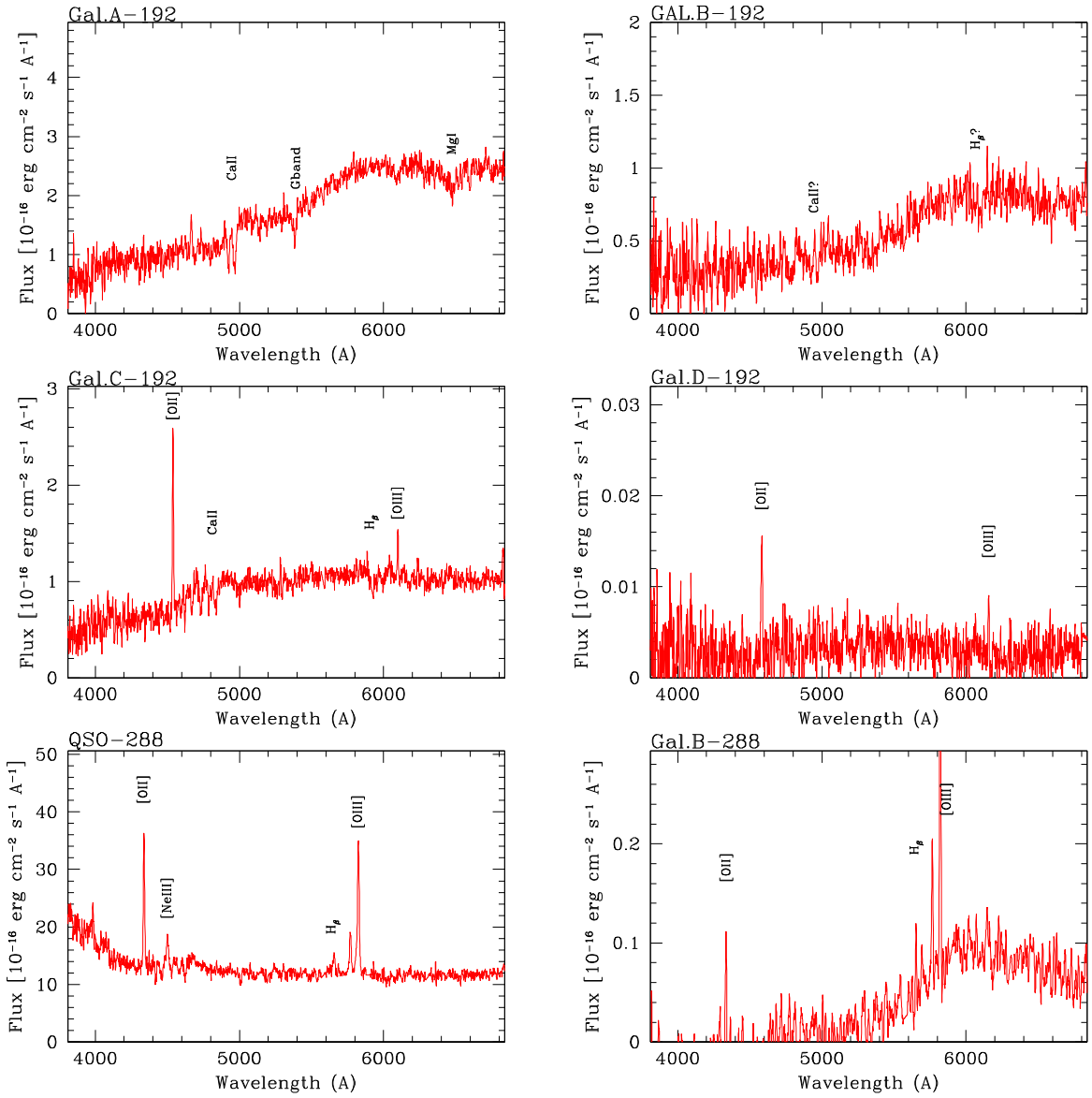

Figure 2 – *continued.*

SFRs are given in Table 2. Since we cannot estimate directly the intrinsic reddening for the observed galaxies from the spectra (e.g. from Balmer decrement), we assume nominal factor of 2 for the ratio of extinction between [O II] and Hα (e.g. Kennicutt 1998) to compute the SFR from Gilbank et al. (2010; equation 8). The adopted relation takes into account the dependence of SFR from dust extinction and metallicity using an empirical relation with the stellar mass (see Gilbank et al. 2010). We find that the SFR for all observed companion galaxies is in the range $\sim$0.02 to $\sim$15 $M_{\odot}$ yr^{-1}. For five companion galaxies associated with the QSO, the median SFR is 1.0 ± 0.8 (error represents the semi-inter-quartile range), while for six that are not associated it is 1.5 ± 0.1. For the QSO host galaxies in nine cases, we detect [O II] emission. For five of them the SFR is modest (<1 $M_{\odot}$ yr^{-1}), while in two cases (QSOs 170 and 192), a high SFR was found ($\sim$10 $M_{\odot}$yr^{-1}) and in one case (QSO 288) we estimate a very high SFR ($\sim$140 $M_{\odot}$yr^{-1}). The specific SFR (sSFR = SFR/M_*) for most of the galaxies in which [O II] emission is detected is much smaller than 1 Gyr^{-1}. This is suggestive of only modest star formation integrated over the Hubble time. Only in few cases a greater sSFR is found that could be due to a recent episode of star formation.

We note that the values of SFR as derived from the [O II] luminosity assume that the observed $L_{[O\,II]}$ luminosity is representative of the whole galaxy. This is a reasonable assumption for most of the companion galaxies because their size is comparable with or somewhat larger than the slit aperture used for the spectra. However, in some cases (e.g. the QSO 288 host; see Fig. 1) the slit aperture intercepts only a fraction of the host galaxy, therefore, any gradient or structured emission may bias this measurement.

4.3 Spectra of the host galaxies

In addition to the optical spectra of the companion galaxies, we secured off slit ($\sim$1–2 arcsec) spectra of the QSO in order to better gather the starlight signal from their host galaxies see Figs 1 and 2. In the cases where more than one companion could be observed in the same slit, the orientation was set to detect two companions (see Table 1).

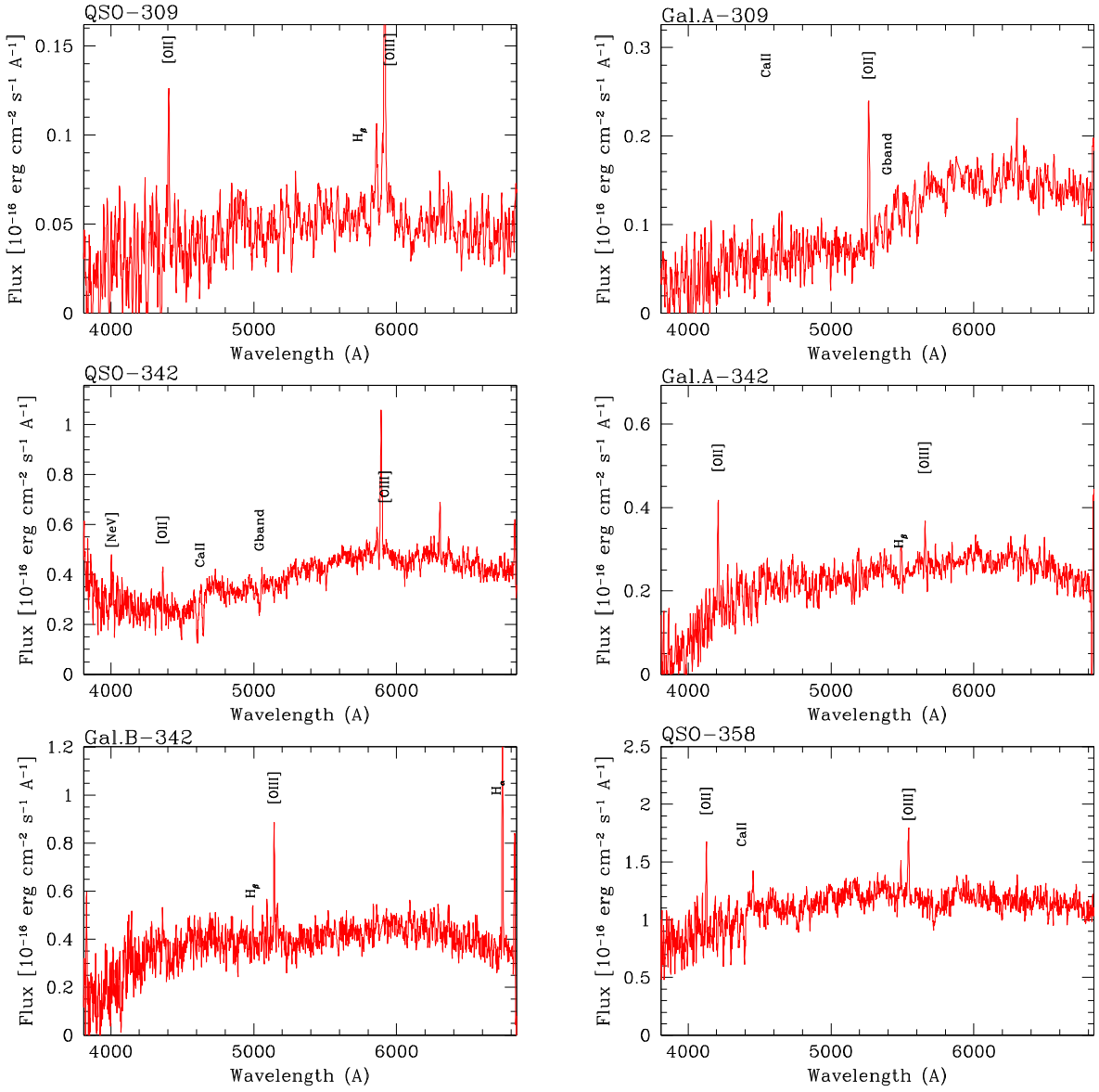

Figure 2 – *continued.*

Depending on the brightness of the nucleus and on the position of the slit, some spectra of the targets (QSO) contain therefore the flux contribution from a fraction of the nucleus light and from the host galaxy. For QSO #40, #342 and #358, we are able to detect the Ca II H, *K*- and *G*-band absorption features from the old stellar population of the QSO hosts (see Fig. 3). In all these cases [O II] 3727 Å emission is also present. Because of the strong emission from the QSO, some contribution of the [O II] flux could be due to the nucleus. However, since [O II] originates mainly in HII regions, the contamination from the nucleus should be unimportant. Note that in two out of these three cases there is also a close companion galaxy associated with the QSO.

5 SUMMARY AND CONCLUSIONS

We obtained optical spectroscopy of 21 close companions galaxies for 12 low-redshift ($z < 0.3$) QSOs. It turns out that 11 of them are associated with the QSO and most of them are at PD < 80 kpc. In two cases, we found that more than one companion galaxy is associated with the QSO. In five cases of associated companions, their spectra exhibit significant [O II] 3727 Å emission. These companions are at PD of 20–50 kpc, therefore if the ionization source is due to the QSO, the companion galaxy occupies a small solid angle as seen from the quasar, and only a small fraction of the ionizing flux will hit the companion. Under these conditions, the [O II] emission-line intensity is directly related to the ionization parameter (c.f. Gnedin 1997) that is significantly reduced by the covering factor ($\sim 10^{-3}$ for a companion of 3 kpc at a distance of 40 kpc). The Equivalent Width (EW) of [O II] lines of these companion galaxies cover a wide range (3–80 Å) and are comparable to the few other spectroscopic measurements of close companion galaxies reported by Gnedin (1997). The average level of star formation (as derived from [O II] luminosity) of companion galaxies that are associated with the QSO appears similar to that of the companion galaxies that are not associated with the QSO. The majority (9 out of 11) of the observed QSO exhibit [O II] emission; however, only in three cases the SFR is significant. Two of them (QSO #170 and #288) have also associated close companions with [O II] emission while in one

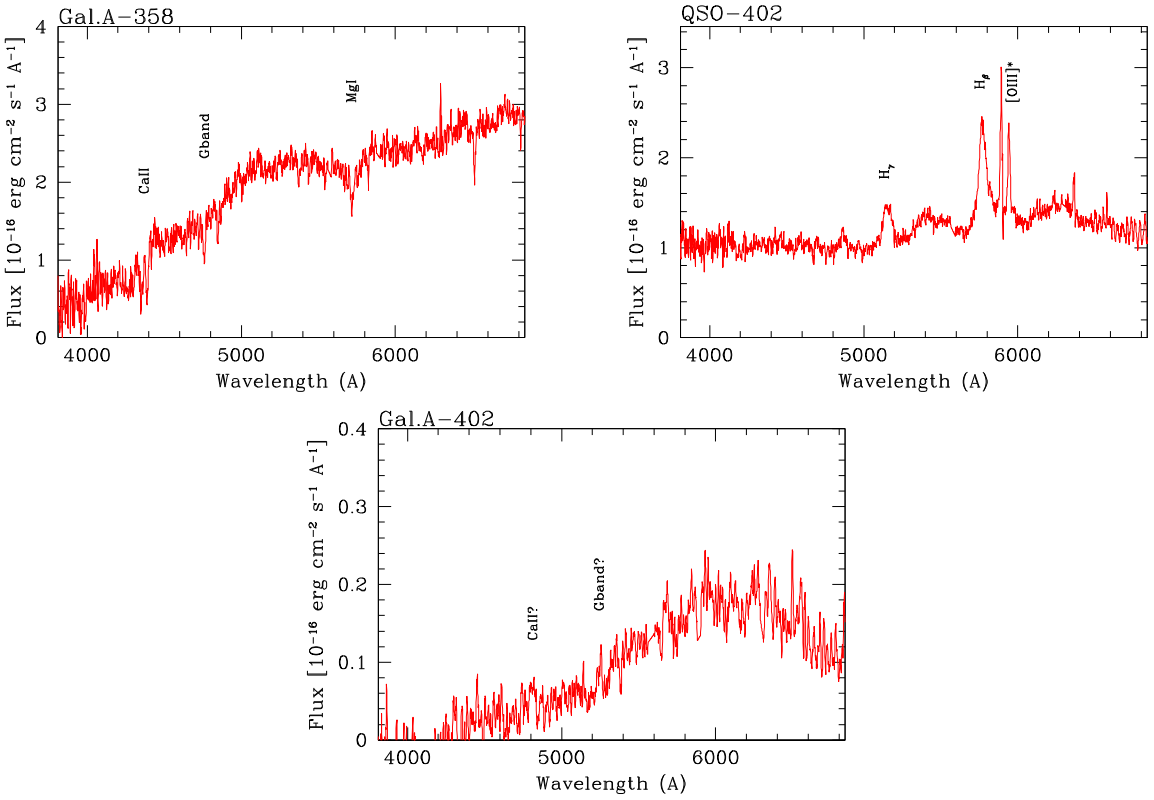

Figure 2 – *continued.*

Table 2. [O II] emission-line measurements.

Obj	z_{our}	log(Flux) (erg s^{-1})	log (L) ($L/L_\odot$)	SFR ($M_\odot$ yr^{-1})	sSFR ($yr^{-1} \times 10^{-10}$)	log(M^*) ($M/M_\odot$)
QSO-36	0.2355	39.86 ± 0.09	6.27	0.5 ± 0.1	0.1	10.66
A	0.1070	40.40 ± 0.06	6.82	0.5 ± 0.05	0.5	10.04
B	0.2356	–	–	–	–	–
QSO-40	0.2338	40.03 ± 0.05	6.44	0.6 ± 0.06	0.1	10.54
B	0.2333	41.22 ± 0.06	7.63	6.9 ±0.07	2.9	10.38
QSO-62	0.2656	–	–	–	–	–
A	0.2873	–	–	–	–	–
QSO-92	0.1686	39.70 ± 0.09	6.11	0.3 ± 0.06	0.1	10.54
A	0.3141	–	–	–	–	–
B	0.1175	40.54 ± 0.05	6.95	1.5 ± 0.15	0.6	10.38
C	0.1687	–	–	–	–	–
QSO-130	0.1853	–	–	–	–	–
A	0.1863	–	–	–	–	–
B	0.1852	40.28 ± 0.35	6.70	0.1 ± 0.01	20.3	7.9
C	0.1855	40.82 ± 0.06	7.24	1.0 ± 0.1	1.5	9.8
QSO-170	0.2590	41.37 ± 0.05	7.78	14.3 ±1.4	3.3	10.64
B	0.2590	40.89 ± 0.06	7.30	6.7± 0.7	0.5	11.13
QSO-192	0.2526	41.26 ± 0.05	7.67	15.3 ±1.5	1.3	11.06
A	0.2178	41.37 ± 0.05	7.78	15.4 ±1.5	3.0	10.71
B	0.2511	–	–	–	–	–
C	0.2295	38.92 ± 0.11	5.34	0.02 ± 0.01	0.01	10.15
D	0.2513	–	–	–	–	–
QSO-288	0.1636	42.27 ± 0.05	8.69	143.7 ± 14.1	18.1	10.9
B	0.1639	40.01 ± 0.12	6.43	0.8 ± 0.08	0.1	10.93
QSO-309	0.182	40.07 ± 0.05	6.48	0.8 ± 0.08	0.1	10.71
A	0.4124	40.95 ± 0.07	7.37	6.1 ± 0.06	1.1	10.76

Table 2 – *continued.*

Obj	z_{our}	log(Flux) (erg s^{-1})	log (L) ($L/L_{\odot}$)	SFR ($M_{\odot}$ yr^{-1})	sSFR ($yr^{-1} \times 10^{-10}$)	log(M^*) ($M/M_{\odot}$)
QSO-342	0.1691	40.02 ± 0.05	6.43	0.7 ± 0.07	0.1	10.69
A	0.1297	40.03 ± 0.07	6.45	0.1 ± 0.01	0.6	9.25
B	0.0273	–	–	–	–	–
QSO-358	0.1070	40.20 ± 0.05	6.61	0.7 ± 0.07	0.3	10.43
A	0.1058	–	–	–	–	–
QSO-402	0.1869	–	–	–	–	–
A	0.2322	–	–	–	–	–

Column (1) identifier from Falomo et al. (2014), column (2) the redshift from our measurements. Column (3) log of the flux of [O II] line (error is obtained combining the uncertainty in the flux calibration based on the SDSS−DR7 photometry and the measurement of line fluxes); column (4) log of the luminosity; column (4) the derived SFR in $M_{\odot}$ yr^{-1}, column (5) specific SFR in yr^{-1} and column (6) the stellar mass in $M_{\odot}$.

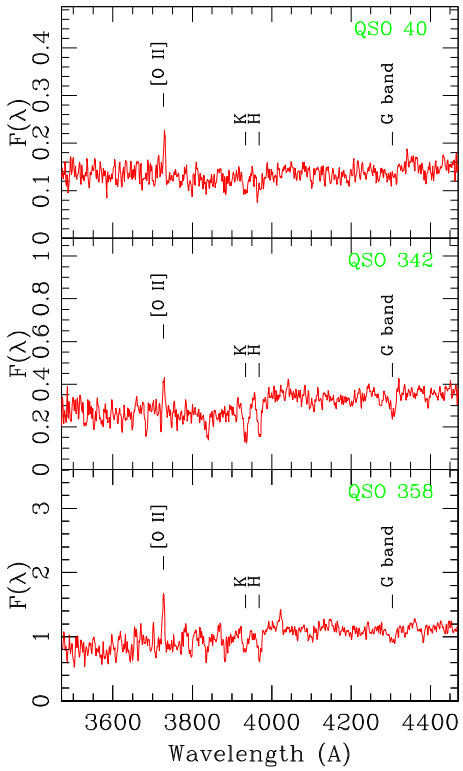

Figure 3. The rest-frame spectra of the QSO host galaxies for targets #40, #342 and #358. Clear signature of the underlying stellar population is apparent. In all cases, a significant [O II] 3727 Å emission line is detected. The spectra were obtained through a slit that was offset from the nucleus (see details in Table 1).

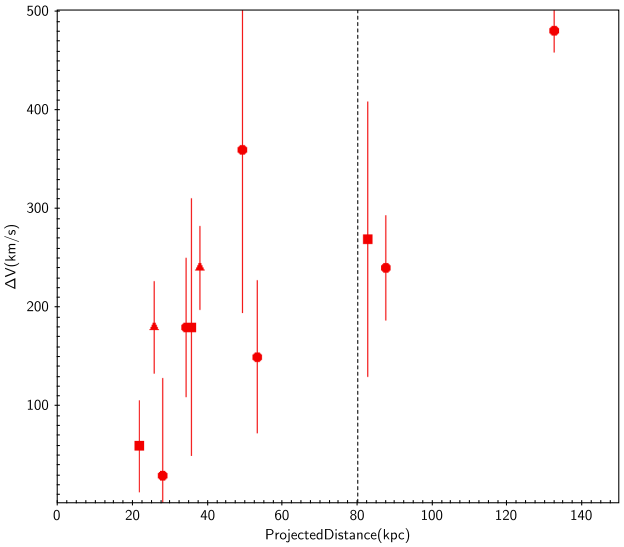

Figure 4. The difference of radial velocity between the QSO and the associated companion galaxy versus the projected distance of the companion. Different symbols refer to QSO with only one companion galaxy (filled circles), with two companion galaxies (filled triangles) and with three companions (filled squares). The dashed vertical line indicates the projected distance of 80 kpc (see text).

case (QSO #192) no [O II] emission in associated companions are found. These results suggest (albeit still based on a scanty statistics) a modest role of the QSO emission for the star formation in nearby companion galaxies.

For three objects, we are also able to detect the starlight spectrum of the QSO host galaxy the spectrum of which is characterized by prominent absorption lines of old stellar population and low level of SFRs (c.f. also Matsuoka et al. 2015).

ACKNOWLEDGEMENTS

We thank the anonymous referee whose comments improved the paper. Funding for the SDSS and SDSS-II has been provided by the Alfred P. Sloan Foundation, the Participating Institutions, the National Science Foundation, the US Department of Energy, the National Aeronautics and Space Administration, the Japanese Monbukagakusho, the Max Planck Society, and the Higher Education Funding Council for England. The SDSS Web Site is http://www.sdss.org/.

The SDSS is managed by the Astrophysical Research Consortium for the Participating Institutions. The Participating Institutions are the American Museum of Natural History, Astrophysical Institute Potsdam, University of Basel, University of Cambridge, Case Western Reserve University, University of Chicago, Drexel University, Fermilab, the Institute for Advanced Study, the Japan Participation Group, Johns Hopkins University, the Joint Institute for Nuclear Astrophysics, the Kavli Institute for Particle Astrophysics and Cosmology, the Korean Scientist Group, the Chinese Academy of Sciences(LAMOST), Los Alamos National Laboratory, the Max-Planck-Institute for Astronomy (MPIA), the Max-Planck-Institute for Astrophysics (MPA), New Mexico State University, Ohio State University, University of Pittsburgh, University of Portsmouth, Princeton University, the United States Naval

Observatory and the University of Washington. Based on observations made with the Nordic Optical Telescope, operated by the Nordic Optical Telescope Scientific Association at the Observatorio del Roque de los Muchachos, La Palma, Spain, of the Instituto de Astrofisica de Canarias.

REFERENCES

Abazajian K. N. et al., 2009, ApJ, 182, 543
Annis J. et al., 2014, ApJ, 794, 120
Bahcall J. N., Kirhakos S., Saxe D. H., Schneider D. P., 1997, ApJ, 479, 642
Bekki K., 1999, ApJL, preprint (astro-ph/9904044)
Bettoni D., Falomo R., Kotilainen J. K., Karhunen K., Uslenghi M., 2015, MNRAS, 454, 4103
Benítez N., Sanz J. L., Martínez-González E., 2001, MNRAS, 320, 241
Blanton M. R., Roweis S., 2007, AJ, 133, 734
Coldwell G. V., Lambas D. G., 2003, MNRAS, 344, 156
Coldwell G. V., Lambas D. G., 2006, MNRAS, 371, 786
Di Matteo T., Springel V., Hernquist L., 2005, Nature, 433, 604
Falomo R., Kotilainen J., Treves A., Carangelo N., 2001, ApJ, 547, 124
Falomo R., Treves A., Kotilainen J. K., Scarpa R., Uslenghi M., 2008, ApJ, 673, 694
Falomo R., Bettoni D., Karhunen K., Kotilainen J. K., Uslenghi M., 2014, MNRAS, 440, 476
Gallagher J. S., Hunter D. A., Bushouse H., 1989, AJ, 97, 700
Gnedin O. Y., 1997, ApJ, 491, 69
Gilbank D. G., Baldry I. K., Balogh M. L., Glazebrook K., Bower R. G., 2010, MNRAS, 405, 2594
Gilbank D. G., Baldry I. K., Balogh M. L., Glazebrook K., Bower R. G., 2011, MNRAS, 412, 2111
Jacoby G. H., Hunter D. A., Christian C. A., 1984, ApJS, 56, 257
Hutchings J. B., 1995, AJ, 109, 928
Hutchings J. B., Morris S. C., 1995, AJ, 109, 1541
Hutchings J. B., Neff S. G., 1992, AJ, 104, 1
Hutchings J. B., Crampton D., Persram D., 1993, AJ, 106, 1324
Hutchings J. B., Crampton D., Johnson A., 1995, AJ, 109, 73
Kalfountzou E., Jarvis M. J., Bonfield D. G., Hardcastle M. J., 2012, MNRAS, 427, 2401
Kauffmann G., Haehnelt M., 2000, MNRAS, 311, 576
Kauffmann G. et al., 2003, MNRAS, 341, 33
Karhunen K., Kotilainen J. K., Falomo R., Bettoni D., Usleghi M., 2014, MNRAS, 441, 1802
Kennicutt R. C., Jr1998, ARA&A, 36, 189
Kewley L. J., Geller M. R. A., Jansen R. A., 2004, AJ, 127, 2002
Matsuoka Y., Strauss M. A., Price T. N., III, DiDonato M. S., 2014, ApJ, 780, 162
Matsuoka Y. et al., 2015, ApJ, 811, 91
Serber W., Bahcall N., Ménard B., Richards G., 2006, ApJ, 643, 68
Shanks T., Boyle B. J., Peterson B. A., 1988, in Osmer P., Phillips M. M., eds., ASP Conf. Ser. Vol. 2, The Spatial Clustering of QSO's. Astron. Soc. Pac., San Francisco, p. 244
Smith R. J., Boyle B. J., Maddox S. J., 2000, MNRAS, 313, 252
Söchting I. K., Clowes R. G., Campusano L. E., 2002, MNRAS, 331, 569
Söchting I. K., Clowes R. G., Campusano L. E., 2004, MNRAS, 347, 1241
Stockton A., 1982, ApJ, 257, 33
Stockton A., MacKenty J. W., 1987, ApJ, 316, 584
Villar-Martín M., Tadhunter C., Humphrey A., Encina R. F., Delgado R. G., Torres M. P., Martínez-Sansigre A., 2011, MNRAS, 416, 262
Wake D. A. et al., 2004, ApJ, 610, L85

APPENDIX: NOTES TO INDIVIDUAL OBJECTS

QSO 36

Radio quiet quasar at $z = 0.2356$ as derived from [O III] emission lines. The optical spectrum of closest companion galaxy (labelled B, $r = 19.1$; distance 53 kpc from the QSO) shows clear absorption features of the Ca II, G band, H_β and MgI 5175 Å at $z = 0.2356$. The chosen slit position intercepts also another compact object (label A) at 33.5 arcsec from the QSO. The slit position was only barely tangent to this object that is classified as star by SDSS. A very faint diffuse companion is present at ∼3 arcsec from object A and intercepted by the slit. Our spectrum is characterized by a blue continuum with emission lines of [O III] and [O II] and stellar absorption features (CaII, G band and Na I) at the redshift $z = 0.107$.

QSO 40

This QSO ($z = 0.2335$) has a very close companion galaxy (labelled B, $r = 20.0$) at 27 kpc PD. Our optical spectrum shows prominent (EW = 63 Å) [OIII] 5007 Å emission line and also very strong [OII] 3727 Å(EW = 71 Å). In addition, we also detect emission of [NeIII] 3869 Å and H_β and Ca II absorptions. All these lines correspond to the redshift $z = 0.2332$ that is identical within the measurement errors ($\Delta V = 150$ km s^{-1}) to that of the QSO. This is thus a clear case of physical association QSO-close companion galaxy with evidence of significant star formation. The slit crosses also object labelled A that is a foreground star.

QSO 62

The QSO ($z = 0.2674$) has a quasi-edge on spiral galaxy (labelled A, $r = 19.7$) at PD = 67 kpc. The spectrum of this companion is characterized only by absorption features (Ca II, G band and H_β) at $z = 0.2868$. The large (∼6000 km s^{-1}) difference of radial velocity excludes a present association with the quasar. At ∼2.5 arcsec (corresponding to PD = 16 kpc) from the QSO there is a fainter ($r = 21.1$) compact companion (labelled B, see Fig. 1) that is only marginally detected by our spectrum.

QSO 92

In the immediate environment of this QSO ($z = 0.1681$) there are two similar galaxies at PD = 72 kpc (B; $r = 18.1$) and PD = 87 kpc (C; $r = 18.7$). Our spectra shows that only galaxy C can be associated with the QSO having a difference of radial velocity of ∼230 kms^{-1}. The other companion galaxy (B) is a foreground object ($z = 0.1175$). Another fainter and closer compact companion (A; see Fig. 1) is instead a background object at $z \sim 0.3$. Also in this case the associated companion galaxy (C), in addition to, absorption lines from the stellar population of the galaxy shows also moderate [O II] 3727 Å emission line (EW = 4.6 Å).

QSO 130

There are two close companions (A,C) at PD of 22 and 35 kpc, respectively. Both companions are at the same redshift ($\Delta V \sim 50$ km s^{-1}) as the QSO ($z = 0.1861$). While companion A has a pure absorption spectrum, the companion galaxy C shows a prominent [O II 3727] emission (EW = 30 Å) and also [O III] 5007 Å and H_β (see Fig. 1). Curiously we found another emission-line galaxy at the same redshift at ∼ 19.5 arcsec W of the QSO (PD = 82 kpc) in the spectrum obtained with the slit oriented along the QSO-gal. A direction (E–W).

QSO 170

The optical spectrum of the spiral companion galaxy ($r = 19.8$; PD = 34 kpc) to this QSO ($z = 0.2596$) shows both absorption lines (Ca II) and again [O II] 3727 Å emission at $z = 0.2595$ ($\Delta V < 100$ km s^{-1} with respect to the QSO).

QSO 192

The immediate environment around this QSO ($z = 0.2519$) is rather complex (see Fig. 1). There are two close companions the closest at ∼ 3.5 arcsec W is a star and the other is a galaxy (labelled B) at ∼6 arcsec NW at a redshift very close to that of the QSO

($z = 0.2511$). We observed this field at two PA (15° and 120°) obtaining the spectra of 3 more close objects (A, C and D) all are galaxies, A and C are foreground objects, while D has a redshift close to the QSO ($z = 0.2513$).

QSO 288

This QSO ($z = 0.1627$) is hosted by a face-on spiral galaxy. The optical spectrum of the closest (object B, PD $\sim$ 50 kpc) faint ($r = 21.3$) companion turned out to be at $z = 0.1627$.

QSO 309

The faint ($r = 20.6$) companion galaxy of this QSO ($z = 0.1823$) at PD = 63 kpc (object A) is a background emission-line galaxy at $z = 0.4129$. The host galaxy shows a faint spiral structure.

QSO 342

There are two companion galaxies (see Fig. 1) that encompass this QSO ($z = 0.1705$) at PD = 123 (A) and PD = 82 (B). Either these companions are foreground emission-line galaxies at $z = 0.1297$ and 0.0273, respectively. Our optical spectrum was secured along the direction (PA = 142°) connecting the companion galaxies A and B (see Fig. 1). With such position we are also able to intersect the flux of the host galaxy of the quasar (at 1.3 arcsec from its centre). The spectrum of the QSO host (see Fig. 1). We detect stellar absorption lines as H, K of Ca II and G band, Mg I 5875 Å, Ca+Fe.

QSO 358

QSO (z = 0.1074) hosted by a spiral galaxy with a tidal tail. We tool the spectrum of the relatively bright ($r = 17.6$) edge-on companion galaxy that is at 133 kpc from the QSO in the direction of the extension of the tidal tail (see Fig. 1). We found a pure absorption line spectrum for this companion that is at $z = 0.1058$. The difference in terms of radial velocity between the companion and the QSO is $\sim$ 500 km s^{-1} thus it is unlikely that they form a bound system but suggests that there was some interaction in the past.

QSO 402

We took the spectrum of the faint ($r = 20.4$) companion object at PD = 56 kpc that turned out to be at $z = 0.2322$.

This paper has been typeset from a TEX/LATEX file prepared by the author.